IOP Conf. Series: Materials Science and Engineering **101** (2015) 012062 doi:10.1088/1757-899X/101/1/012062

# Experimental study of stability and transients in a horizontally heated boiling helium thermosyphon

**H Furci***, **A Four**, **B Baudouy**

CEA Saclay, Irfu/SACM, 91191 Gif-sur-Yvette, France

*Corresponding author: *hernanfurci@gmail.com*

**Abstract.** Experiments were conducted on a liquid helium natural circulation loop with a 4 m long horizontal heated section. Wall temperatures on the heated section, mass flow rate and pressure drop were measured in steady and transient regimes. The stability of the loop has been studied and the power stability limits have been found. Also, different heating configurations were explored and their drawbacks and benefits were observed. The result is that the loop is stable only above a non-zero low power and below a certain upper power limit. The distance from the heating to the vertical riser affects the stability range. It has been found that instabilities at low power or transients following a low power step pulse can produce considerable temperature oscillations, potentially dangerous from the magnet protection point of view.

## 1. Introduction

Natural circulation loops are used as cooling systems in superconducting magnet devices. Examples are the CMS at CERN [1, 2] or R3B-GLAD for GSI [3]. Within the R&D program for the design of the R3B-GLAD spectrometer [4], a study of boiling helium natural circulation loops with horizontal heated sections was started, with the aim of validating this cooling method. In that opportunity the operation of the system was only studied at very low heat input, corresponding to the design requirements. Later, a study was conducted on a wider power range so as to characterize the steady state operation, experimentally and theoretically [5].

In this work we push further the study by investigating the operation regimes that are not steady; either resulting from the fact that the equilibrium of the system is unstable, or from the response to a time varying heat load.

## 2. Experimental setup

The experiments were conducted in the same experimental facility as those presented in references [4, 5] with some modifications. The loop, schematized in figure 1, is composed of an upper liquid helium reservoir and a U-shaped circuit below it. The reservoir, with 50 l capacity, acts as a phase separator. From its bottom descends a 1.4 m long, 4 cm diameter tube, *the descending section*. Then, a horizontal section reduces diameter and connects it to the *ascending section*. The latter is formed by three elements: a *short vertical section* (non-heated, 17 cm long), a horizontal spirally arranged 5 m long tube —which will receive special attention in the next paragraph— and another long vertical section (1.1 m) that we will call *riser* and reenters the bottom of the reservoir. The whole is inside a 2 m deep well cryostat, with a liquid nitrogen shield, reflective aluminum screens and continuous vacuum pumping.

Content from this work may be used under the terms of the Creative Commons Attribution 3.0 licence. Any further distribution of this work must maintain attribution to the author(s) and the title of the work, journal citation and DOI.
Published under licence by IOP Publishing Ltd

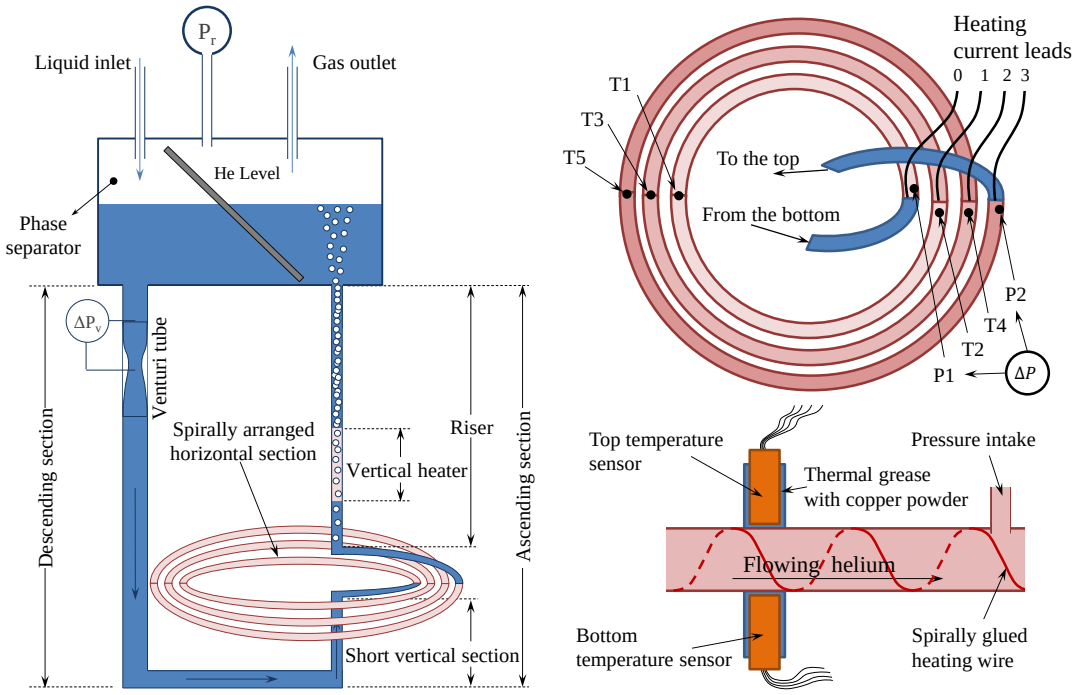



**Figure 1.** Experimental setup diagrams. Left: the elements of the loop; right top: the horizontal section with its instrumentation points; right bottom: the position of the temperature sensors on the tube and the pressure intakes.

**Table 1.** Geometrical parameters of the test section: positions of the temperature and pressure intakes and heating lengths in the 3 configurations. All length in meters.

| T1 | T2 | T3 | T4 | T5 | P1 | P2 | L(0-1) | L(0-2) | L(0-3) |
|---|---|---|---|---|---|---|---|---|---|
| 0.613 | 1.318 | 1.968 | 2.738 | 3.440 | 0.018 | 4.255 | 1.318 | 2.738 | 4.273 |

The horizontal section of the loop is the *heated section*, shown in figure 1 on the top right; of its 5 m length, 4.27 m can be heated by a spirally glued wire on its external wall (lighter color in the figure). The section is arranged in 3 turns, and the heating can be independently set on one, two or the three of the turns by choosing two of the four current leads (current lead 0 plugs at the entrance of turn 1 and 1, 2 and 3 at the exit of the respective turns). Before the entrance (at the inner turn) and after the exit (outer turn), there are short non-heated horizontal sections (of around 40 cm length). The experiments are conducted by controlling the power applied to the horizontal heated section and on which turns it is applied. The long vertical section has a 17 cm long region that can be heated by a spirally glued wire too. This allows modifying the mass flow rate of the circuit without acting on the main power supply.

Internal wall temperature is measured non-intrusively by placing Lake Shore Cernox AA sensors on the exterior of the heated sections. This can be done because the material of the test section is hyper pure copper, with RRR of 145, and the thermal conductivity and diffusivity are extremely high. There are five couples of temperature sensors placed at the five positions given in table 1 and shown in figure 1. For each couple, one of the sensors is at the bottom of the tube and the other is at the top, to see if phase stratification could induce heat transfer differences. The total mass flow rate is measured with a Venturi tube on the descending section.

**Table 2.** Loop stability power limits. NHHL: non-heated horizontal length after the heated section.

| Configuration | NHHL (m) | Lower limit (W) | Upper limit (W) |
|---|---|---|---|
| 0-3 | 0.360(10) | 1.2(4) | 78(3) |
| 0-2 | 1.895(10) | 2.8(4) | 71(2) |
| 0-1 | 3.315(10) | 3.7(2) | 60(1) |

The Venturi pressure drop and the heated section pressure drop are measured with Validyne differential pressure transducers DP1020 and DP1022, respectively.

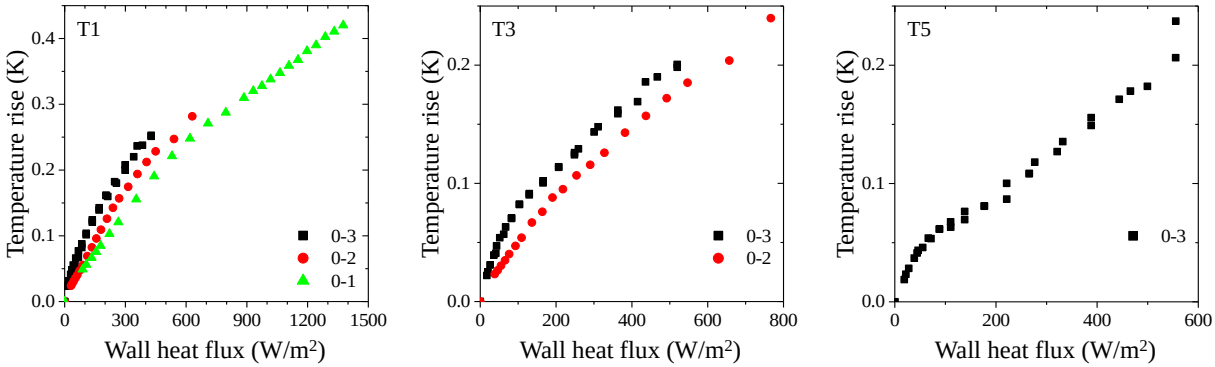
The loop was studied for three heating configurations: configuration 0-3: the three turns are heated; configuration 0-2: only the first and second turns are heated; configuration 0-1: only the first turn is heated. The identification numbers refer to the current leads used for the electrical connection of the heater (see figure 1). Thus, the heating configurations differ only in the distance from the end of the heated section to the vertical riser.

## 3. Steady natural circulation and stability limits

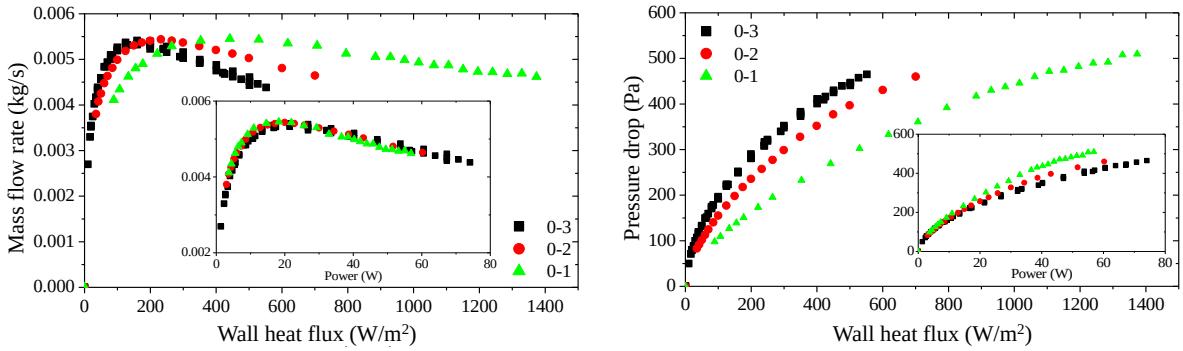
The first study consisted in applying a quasi-steadily increasing power to the heated section, i.e. increasing gradually at small steps. At very low power, it was not possible to achieve a stable circulation. The system would exhibit regular mass flow rate bursts, as had already been reported before [4]. The effect was more pronounced with heating configurations 0-1 and 0-2, as the required power for stability was higher. Once the steady condition at steady power was achieved, the mean values of wall temperature, mass flow rate and heated section pressure drop were recorded as a function of power. The values thus obtained are presented in figure 2 as a function of applied heat flux. In order to be able to compare the three configurations, inlet mass flow rate $\dot{m}$ and pressure drop $\Delta P$ are also plotted as a function of applied total power. At a certain power value, this time high, the system became unstable again, i.e. a growing oscillating perturbation appears on mass flow rate and the other variables. Thereafter, the time dependent signals were recorded instead. Thus, there are two stability limits, a lower one and an upper one. Stability limits for the three configurations are presented in table 2. The system is stable (constant mass flow rate) in between these values.

Within the stability power range, it is remarkable that the mass flow rate of the loop shows no appreciable difference between heating configurations, as a function of the total heating power. The $\dot{m}$ dependence on heat flux shows an increase at low power, a maximum and then a decrease. At low power, it is the buoyant force which is the more responsive to the heat flux, producing the $\dot{m}$ increase. At high power, resistive forces (friction and acceleration gradients) increase strongly with $q$ (mainly due to the increase in quality) while the gravity term varies only slightly (void fraction varies slowly as a function of quality when quality is high). This results in a decrease of $\dot{m}$. $\Delta P$ is slightly higher for identical total power as the heating is concentrated in a shorter region at the entrance. This results in the increase of local velocity at every point of the horizontal section and riser, which in time increases the friction pressure drop. However, these differences are not high enough to produce a significant effect on mass flow rate.

The wall temperature evolutions show that within the stable region no boiling crisis (dry wall heat transfer regimes) happens. The values are typical of nucleate boiling helium flow in ducts [6, 7]. The differences between configurations are not significant, and are presumably due to the fact that at a given wall heat flux $\dot{m}$ varies from one configuration to another.




(a) Temperature evolution at T1, T3 and T5 in heating configurations 0-3, 0-2 and 0-1.




(b) Mass flow rate and pressure drop evolution for the three configurations.

**Figure 2.** System evolution in steady state.

## 4. The unstable oscillations

Outside the stability limits, it was not possible to observe a steady behavior of the loop. Instead, periodic oscillations were observed. The oscillations are not sinusoidal, but consist of an alternation of periods of apparent hydraulic stability with regular mass flow rate bursts ($\dot{m}$-bursts). This puts forward the strong non-linear nature of the phenomenon.

Examples of this behavior for the low power instabilities is presented in figure 3. At low power, the exit quality is strongly influential on density. Furthermore, the equilibrium mass flow rate is low, which results in long transit time. The instabilities are the result of an important transport delay of quality perturbations in response to inlet velocity perturbations from the horizontal heated section, where vapor is produced, to the vertical section of the loop, where it acts on the buoyant force. For example, a positive perturbation in velocity produces a quality decrease front in the heated section that travels at the velocity of the flow. While the front has not reached the riser, no significant effect on the velocity is observed, but as soon as that happens, the buoyant force diminishes, which will induce a quality increase front. When this one reaches the riser, a $\dot{m}$ peak may happen, which will result in a new low quality front. For long time delays (at low power), the alternation of low and high quality regions may be amplified and at some point, the loop could be completely at rest (no inlet velocity), thus accumulating vapor in the heated section. When the vapor reaches the riser, a $\dot{m}$-burst takes place, until the horizontal section is clean of vapor. The high speed of the burst results in an extremely low quality front, so the inlet velocity will quickly decrease to zero again, and the process restarts.

In the high power instability cases, the more influential forces on mass flow rate evolution are the resisting friction and acceleration pressure gradients. The equilibrium mass flow rate diminishes with heat flux, in order to increase quality and produce a greater buoyant force to counterbalance the resisting terms. The friction and acceleration terms can respond immediately

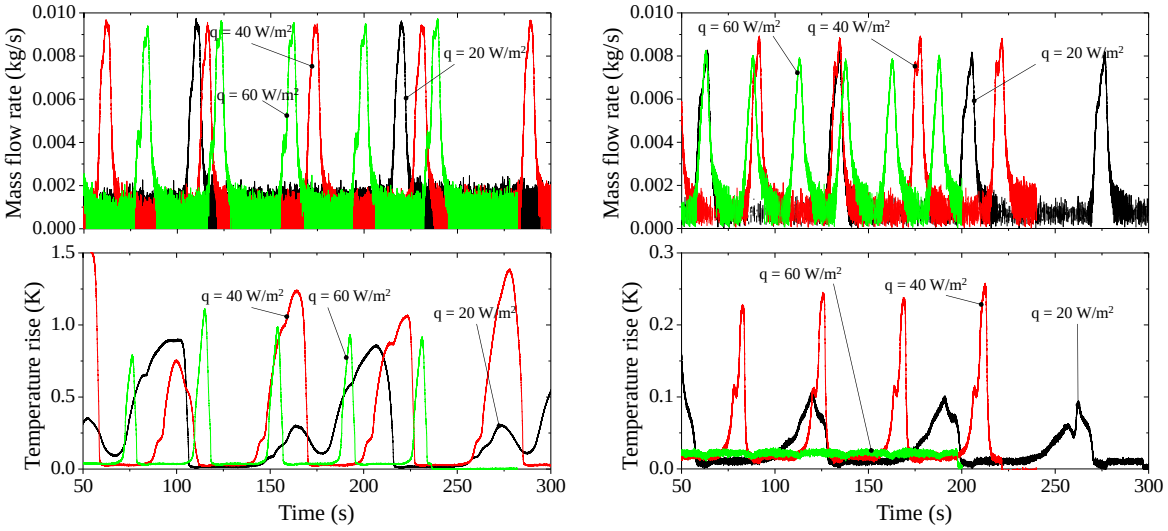



**Figure 3.** Periodic instabilities at low power. Left: configuration 0-2; right: configuration 0-1. The presented temperatures are measured at T1.

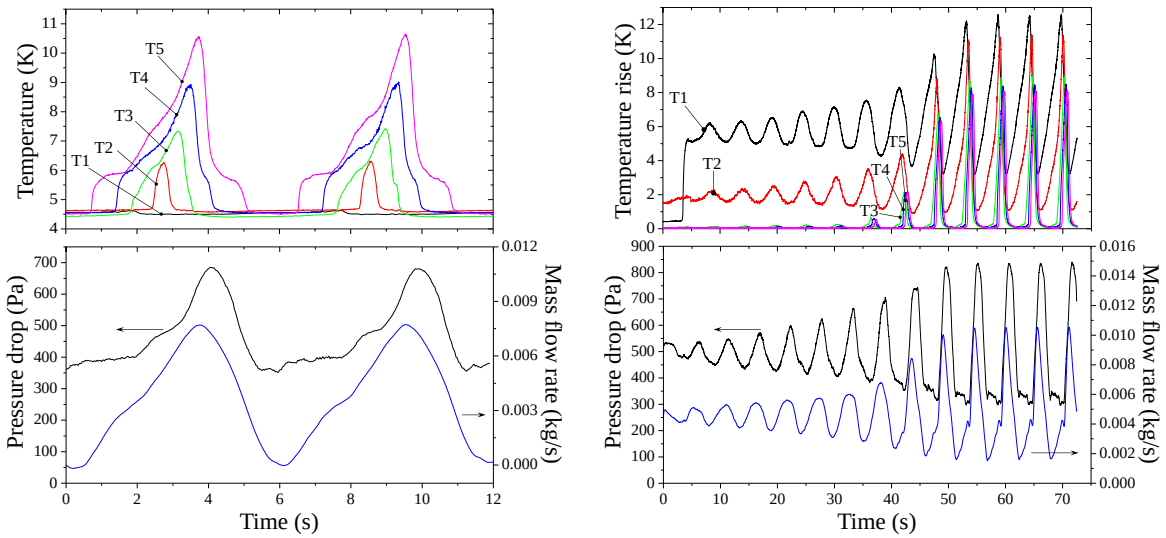



**Figure 4.** Limit cycles of the high power instability. Left: configuration 0-3, $q = 750$ W/m$^2$; right: configuration 0-1, $q = 1465$ W/m$^2$.

to inlet velocity perturbations, but the gravity term presents a transport lag. At a certain power at which the resisting forces' influence is dominant, this lag between opposing forces produces instability. The time evolution of the variables in this kind of instability are shown in figure 4. In the case on the right it is possible to observe how the system amplifies the perturbation away from the equilibrium point. Initially, the growth of $\dot{m}$ is that of a linear second order system (exponentially modulated sinusoidal), but when the size of oscillations is too high the behavior becomes periodic. In dynamic systems jargon, the equilibrium point is linearly unstable and there exists a limit cycle attractor. Some experimental limit cycles in the phase space $(\dot{m}, \frac{d\dot{m}}{dt})$ are shown in figure 5. In particular, for the case of configuration 0-3 we can appreciate how the limit cycles amplitude increases as power increases.

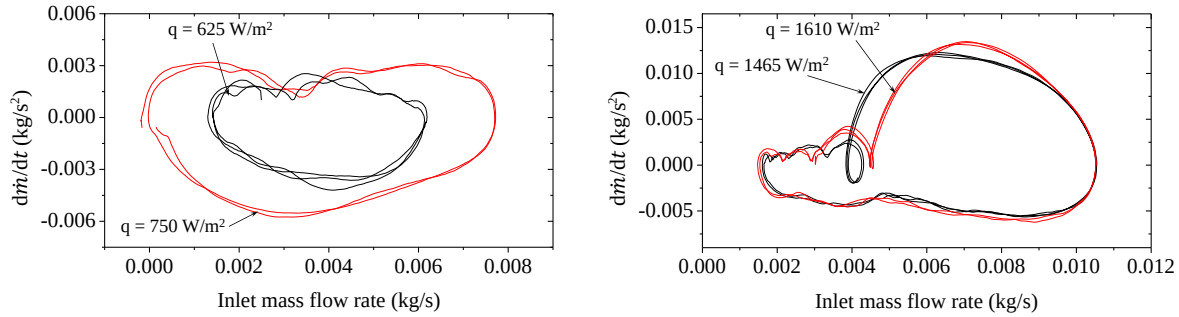



**Figure 5.** Limit cycles in the phase space $(\dot{m}, \frac{d\dot{m}}{dt})$. Left: configuration 0-3; right: configuration 0-1.

## 5. Transient response to power steps

The time response of the loop to a varying heat load was studied by applying a power step pulse on the horizontal heated section, with the system initially at rest ($q = 0$). The time evolution of the measured variables was recorded. The general behavior of the loop in response to this kind of solicitation consists of two distinct stages. Initially, there is a stage of *vapor accumulation in the horizontal section*, during which the produced vapor is not capable of creating buoyant force. During this lapse of time there is no appreciable inlet flow. However, it is presumable that phase change expansion will produce a velocity gradient from the entry towards the exit of the heated section and that phase stratification will be more marked where velocity is low, i.e. near the entrance. This movement will originate the second stage of the transient: vapor reaches the vertical riser and creates buoyant force. At this point, natural circulation (positive inlet flow) starts. If the applied power is in the stability range then the flow may oscillate before finally reaching the steady state. Otherwise, the oscillations will conduce to the limit cycles.

The duration of the first stage is directly determined by the transit time of vapor to the riser. The length of the horizontal section, specially the non-heated length downstream the heated section, plays a significant role. Furthermore, heat transfer in the two stages is substantially different. The presence of low velocity at the entrance of the heated section in the initial stage and the consequent stratification can be very critical with respect to the steady state operation. In the following section we will present a particular case that can have harmful consequences from the magnet protection point of view.

## 6. Low power, high temperature excursions

A singular situation was observed at relatively low heat flux. The stepwise application of a heat flux on the system initially in static condition (no heat flux applied) can produce a dangerous temperature evolution. Dangerous in the sense that if in steady state at this heat flux only nucleate boiling regime had been observed, during the transient the wall temperature goes to very higher values during some period of time, up to a few Kelvins. Examples of this situation are presented in figure 6, where a low heat flux of 100 W/m$^2$ was applied in stepwise manner in two configurations.

The deterioration of the heat transfer on the heated section, manifested by an appreciable temperature excursion, may be explained by the stratification of the flow during the first stage of the transient. During this stage, there will be a non uniform stratified flow driven by the vapor leaving the heated section, with zero velocity at the entrance of the heated section (the measured inlet mass flow rate is zero). For this reason, the stratification effects are the highest in this region and, at some point, with void fraction increase the most of the perimeter here is dry. The perimeter-averaged heat transfer coefficient drops; furthermore, the vapor may overheat,

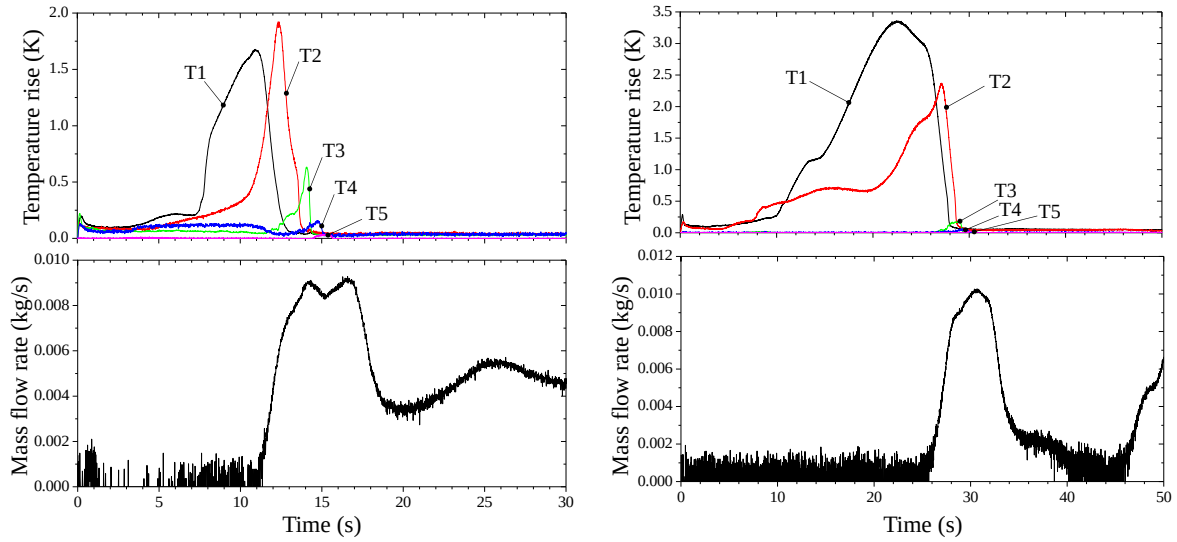



**Figure 6.** Examples of low heat flux, high temperature excursions. Left: $q_f$ = 100 W/m$^2$, config. 0-2; right: $q_f$=100W/m$^2$, config. 0-1.

i.e. saturation thermal equilibrium may be lost. This is actually observed by the temperature increases in the non heated region after the $\dot{m}$-burst, in figure 6 at the right. This onsets wall overheating. Then, the second stage starts when vapor reaching the riser triggers a $\dot{m}$-burst by hydrostatic unbalance. This will promote a cold front from the down-comer into the heated section, and also, the speed increase will promote mixing, breaking phases stratification. That is why, when the mass flow rate appears, the high temperature excursion ends with a transport delay proper to each temperature measurement position.

The effect of the constant presence of a mass flow rate during the first stage of the transient was studied. A flow was created using the auxiliary heating in the riser; the control parameter was the electrical current in the heating wire, which has a 2 Ω resistance. The results of this experiment are shown in figure 7. A significant mitigating effect on the temperature excursion was observed as the auxiliary heating power (and $\dot{m}$) was increased. The highest power value is 0.45 W (for I=0.5 A) and initial $\dot{m}$ values are below 1.5 g/s. At such low $\dot{m}$ values the Venturi flow-meter gives a very low pressure drop ($\approx$ 1 Pa), reason why $\dot{m}$ is difficult to measure. However, the heated section pressure drop is more sensitive and shows unequivocally increasing values in the first stage as the current is increased, confirming the presence of flow. With the increase of heating current, a diminution of the maximum temperature during the transient is observed up to the point of complete attenuation of the excursion at 500 mA of heating current (0.45 W). This effect is a combination of the permanent presence of flow —that promotes mixing and delays the onset of heat transfer deterioration (see the temperature plots)— and the anticipation of the $\dot{m}$-burst due to the diminution of vapor transit time to the riser on the non-heated section (see the $\dot{m}$ plot)—that puts an end to the excursion—.

## 7. Conclusions

The dynamics of a horizontally heated, boiling helium, natural circulation loop have been studied. It has been demonstrated that this kind of system presents important non-stable behavior at too low or too high heating power. The stability limits are sensitive to the non-heated horizontal length downstream the heated section. Instabilities manifest by the dynamics diverging from the equilibrium point towards a limit cycle, which depends on the applied power. These instabilities can present at some moment of the oscillations very low mass flow rates. This

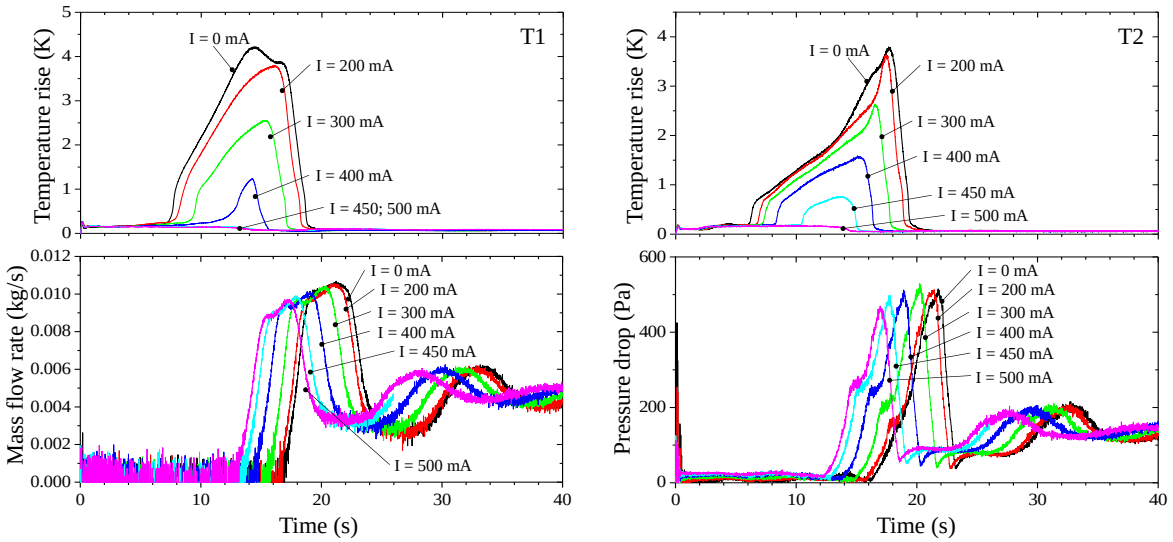



**Figure 7.** Mitigation of low heat flux, high temperature excursions by vertical heater current. Configuration 0-1; $q_f = 150$ W/m$^2$; top left: T1; top right: T2; bottom left: $\dot{m}$; bottom right: $\Delta P$.

can have adverse effects on heat transfer, such as the onset of boiling crisis at low power. This can happen too in the case of the stepwise application of a low heat flux. The lag between the step pulse and the start of the circulation allows the fluid to stratify, which conduces finally to a heat transfer deterioration. It has been shown that the resulting temperature excursions can be harmful from the superconducting magnet protection margins viewpoint. However, the constant presence of a low mass flow rate has been shown to be a good solution for avoiding the undesired phenomenon.

## References

[1] Bredy P, Juster F P, Baudouy B, Benkheira L and Cazanou M 2006 Experimental and theoretical study of a two phase helium high circulation loop *Advances in Cryogenic Engineering, Vols 51A and B* (*AIP Conference Proceedings* vol 823) pp 496–503 Cryogenic Engineering Conference 2005, Keystone, CO, AUG 29-SEP 02, 2005

[2] Baudouy B 2002 Heat and mass transfer in two-phase HeI thermosiphon flow *Advances in Cryogenic Engineering* (*AIP Conference Proceedings* vol 47) pp 1514–1521

[3] Gastineau B, Mayri C, Baudouy B, Berriaud C, Disset G, Donati A, Ducret J E, Eppelle D, Fazilleau P, Graffin P, Jannin J L, Loiseau D, Lottin J P, Massinger M, Pes C, Queinec Y, Sun Z, Charon P, Contrepois P and Neyrial H 2010 *IEEE Transactions on Applied Superconductivity* **20** 328–331 21st International Conference on Magnet Technology (MT-21), Anhui, PEOPLES R CHINA, OCT 18-23, 2009

[4] Gastineau B, Baudouy B, Berriaud C, Bessette A, Bouziat D, Fazilleau P, Graffin P, Hervieu B, Le Bigaut M, Massinger M, Mayri C, Medioni D, Polinski J and Wone M 2012 R3B-Glad Magnet R&D Tests Program: Thermosiphon Loop With Horizontal Section, Superconducting Cable Joints at 3600 A, and Reduced Scale "Coil in its Casing" Mock-Up *IEEE Transactions on Applied Superconductivity* vol 22 22nd International Conference on Magnet Technology (MT), ITER Org, Marseille, FRANCE, Sep 12-16, 2011

[5] Baudouy B, Bessette A and Four A 2013 *Cryogenics* **53** 2–6

[6] Furci H, Baudouy B, Four A and Meuris C 2014 Transient Boiling in Two-Phase Helium Natural Circulation Loops *Advances in Cryogenics Engineering* (*AIP Conference Proceedings* vol 1573) pp 1490–1497 Joint Conference of the Transactions of the Cryogenic Engineering Conference (CEC) / Transactions of the International Cryogenic Materials Conference, Anchorage, AK, JUN 17-21, 2013

[7] Benkheira L, Baudouy B and Souhar M 2007 *International Journal of Heat and Mass Transfer* **50** 3534–3544